HHS Public Access

Author manuscript

J Nutr Biochem. Author manuscript; available in PMC 2023 July 01.

Published in final edited form as:

J Nutr Biochem. 2022 July ; 105: 108998. doi:10.1016/j.jnutbio.2022.108998.

Piceatannol Antagonizes Lipolysis by Promoting Autophagy-Lysosome-Dependent Degradation of Lipolytic Protein Clusters in Adipocytes

Jung Yeon Kwon[1,2,3,#], **Jonathan Kershaw**[1,4,#], **Chih-Yu Chen**[1,5], **Susan M. Komanetsky**[6,7], **Yuyan Zhu**[1,8], **Xiaoxuan Guo**[9], **Phillip R. Myer**[1,10], **Bruce Applegate**[1,11], **Kee-Hong Kim**[1,*]

[1]Department of Food Science, Purdue University, West Lafayette, IN, USA

[2]Department of Food Science and Technology, Oregon State University, Corvallis, OR, USA

[3]Seafood Research and Education Center, Oregon State University, Astoria, OR, USA

[4]Department of Public and Allied Health, Bowling Green State University, Bowling Green, OH, USA

[5]Laboratory for Lipid Medicine and Technology, Harvard Medical School and Massachusetts General Hospital, Charlestown, MA, USA

[6]Department of Nutrition Science, Purdue University, West Lafayette, IN, USA

[7]USDA ARS Grand Forks Human Nutrition Research Center, Grand Forks, ND, USA

[8]Department of Applied Biology and Chemical Technology, Hong Kong Polytechnic University, Hung Hom, Hong Kong, China

[9]Institue of Quality Standard and Testing Technology for Agro-Products, Chinese Academy of Agricultural Sciences, Beijing 100081, China

[10]Department of Animal Science, University of Tennessee, Knoxville, TN, USA

[11]Department of Biological Sciences, Purdue University, West Lafayette, IN, USA

Abstract

Overly elevated circulating non-esterified fatty acids (NEFAs) is an emerging health concern of obesity-associated energy disorders. However, methods to reduce circulating NEFAs remain elusive. The present study determined the effect of piceatannol, a naturally occurring stilbene, on adipocyte lipolysis and its underlying mechanism. Differentiated 3T3-L1 adipocytes, brown

* **Corresponding author**: Kee-Hong Kim, 745 Agriculture Mall Drive, Department of Food Science, Purdue University, West Lafayette, IN 47907, USA, keehong@purdue.edu; Tel.: +1-765-496-2330; Fax: +1-765-494-7953.

#These authors contributed equally to this work

Author Statement

JYK, JK, and CYC conducted experiments, analyzed data, and wrote the manuscript. SMK, YZ, XG and BA conducted experiments and analyzed the data. KHK designed, analyzed, and supervised the research and wrote the manuscript.

Conflict of interest: The authors declare no conflict of interest.

adipocytes and isolated white adipose tissue were treated with various concentrations of piceatannol for 1.5-hr both in the basal and stimulated lipolysis conditions. Piceatannol significantly inhibited NEFAs and glycerol release with a concomitant reduction of ATGL, CGI-58 and PLIN1 expression in adipocytes. Using a series of inhibitor assays, piceatannol-induced degradation of these proteins was found to be mediated by upregulation of the autophagy-lysosome pathway. Moreover, we demonstrated that piceatannol is capable of stimulating autophagy *in vitro*. Importantly, piceatannol administration tended to lower fasting-induced serum glycerol levels in healthy mice. Furthermore, piceatannol administration lowered lipolysis, central adiposity and hyperinsulinemia in diet-induced obese mice. Our study provides profound evidence of a novel inhibitory role of piceatannol in lipolysis through autophagy-lysosome-dependent degradation of the key lipolytic proteins in adipocytes. This study offers a mechanistic foundation for investigating the potential of piceatannol-containing foods in reducing lipolysis and its associated metabolic disorders.

Graphical Abstract

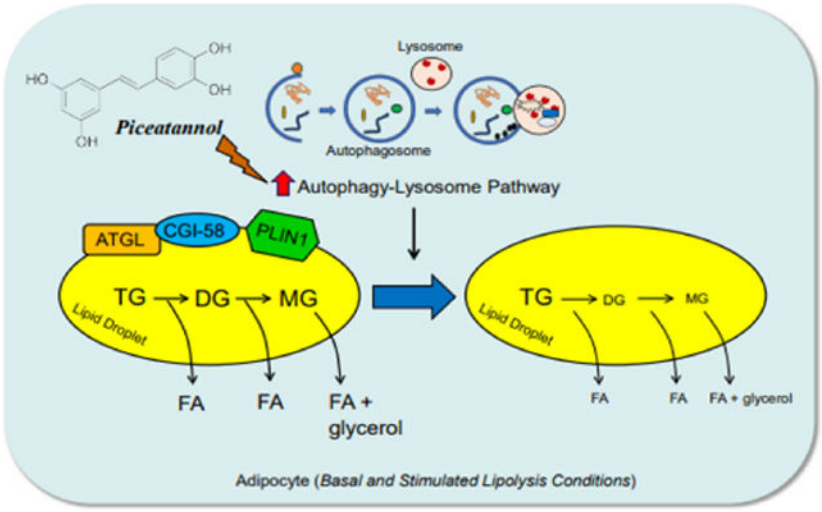

Keywords

adipocytes; ATGL; autophagy; degradation; lipolysis; piceatannol

1. Introduction

Elevated levels of circulating non-esterified fatty acids (NEFAs) is an emerging health concern due to their contribution to the development of obesity-associated insulin resistance and hepatic lipid dysregulation [1, 2]. Overly activated adipose lipolysis is known to promote FA overloading to the peripheral tissues, thereby impairing the metabolic function of these tissues. However, methods to reduce adipose lipolysis to lower circulating NEFAs remain elusive. During periods of energy demands such as starvation and physical exercise, adipocytes hydrolyze their stored triacylglycerol (TG) to NEFAs and glycerol by activation of lipolysis. Lipolysis in adipose tissue requires three major enzymatic steps. Adipose triglyceride lipase (ATGL)/desnutrin/patatin-like phospholipase domain-containing protein

2 (PNPLA2) [3–5] catalyzes the first step of lipolysis for the conversion of TG to diacylglycerol (DG); hormone-sensitive lipase (HSL) then catalyzes the hydrolysis of DG to monoacylglycerol (MAG) which is further hydrolyzed to NEFAs and glycerol by MAG lipase (MAGL). Among these enzymes, adipose-specific ATGL catalyzes the rate-limiting step of lipolysis by binding to a coactivator protein, comparative gene identification-58 (CGI-58)/α/β hydrolase domain-containing 5 (ABHD5) [6], for its maximum lipolytic activity on lipid droplets (LDs) [7]. This association between ATGL and CGI-58 is coordinately regulated by the LD-bound protein perilipin1 (PLIN1), as protein kinase A (PKA)-dependent phosphorylation of PLIN1 releases CGI-58 upon lipolytic stimulation.

Altered ATGL expression and activity cause perturbed lipolysis and NEFA levels, result in several metabolic consequences. Overly activated lipolysis is often associated with obesity-related insulin resistance and hepatic dyslipidemia due to elevated NEFA fluxes and ectopic lipotoxicity [8]. Conversely, *ATGL* deficient mice showed protection from high-fat diet (HFD)-induced insulin resistance [7, 9, 10]. However, *ATGL* deficiency is suggested to be associated with cardiac dysfunction [7], islet β-cell dysfunction [11], impaired brown adipose tissue function [10], and/or premature death [7]. Although complete deficiency of lipolysis results in unfavorable physiological effects, partial inhibition may induce metabolic benefits. For instance, pharmacological inhibition of ATGL activity [12, 13] and genetic ablation of *HSL* or inhibition of HSL activity [14] have shown to be an attractive approach to reduce lipolysis with few metabolic defects.

Piceatannol, a resveratrol analog, is found in various fruits and vegetables such as grapes, blueberries, and passion fruit. Despite a well-documented role of resveratrol in the prevention of obesity [15, 16], evidence of piceatannol's mechanistic role in health is largely limited to its anti-cancer, anti-oxidative and anti-inflammatory properties, primarily as a result of its inhibition of phosphoinositide 3-kinase (PI3K), spleen tyrosine kinase (SYK), nuclear respiratory factor-1 (NRF-1) and nuclear factor-κB (NF-κB)-mediated gene expression [17]. Thus, due to piceatannol's structural similarity to resveratrol, we previously investigated its potential role in lipid metabolism and demonstrated an inhibitory effect of piceatannol in adipogenesis *in vitro*. We also found that the anti-adipogenic effect of piceatannol is largely attributed to inhibition of mitotic clonal expansion and insulin signaling in the early phase of adipocyte differentiation [18]. In addition, we reported that piceatannol suppresses fat accumulation through inhibition of *SBP-1*-dependent lipogenesis [19], and promotes *DAF-16*-dependent lifespan [20] in *Caenorhabditis elegans*. Considering the central role of lipolysis in energy homeostasis and the documented effects of piceatannol in adipocyte metabolism, we hypothesized a role of piceatannol in lipolysis regulation.

In the present study, we demonstrate that piceatannol exhibits an anti-lipolytic effect in adipocytes. We further uncover that the anti-lipolytic effect of piceatannol is primarily attributed to autophagy-induced lysosomal degradation of ATGL, CGI-58, and PLIN1. Moreover, acute administration of piceatannol lowered adipose mass and circulating levels of insulin and leptin in high-fat diet-induced obese mice. Overall, our data suggest that piceatannol is a novel lipolysis inhibitor that promotes autophagy-lysosome system-induced degradation of lipolytic protein clusters.

2. Materials and Methods

2.1. Materials and reagents

Piceatannol was purchased from Alexis Biochemicals (Lausen, Switzerland). Dexamethasone (DEX), 3-isobutyl-1-methyl-xanthine (IBMX), and insulin were obtained from Sigma-Aldrich (St. Louis, MO). Fetal calf serum (FCS) and fetal bovine serum (FBS) were purchased from PAA (Dartmouth, MA). Dulbecco's modified Eagle's medium (DMEM), penicillin/streptomycin, and sodium pyruvate were obtained from Invitrogen (Carlsbad, CA). Protein assay kit was obtained from Bio-Rad Laboratories (Hercules, CA). Antibodies against ATGL, pHSL, Atg7, p62, and LC3 were obtained from Cell Signaling Technology (Beverly, MA). Antibodies for HSL, PLIN1, CGI-58, β-actin, rabbit, and mouse secondary were purchased from Santa Cruz Biotechnology (Santa Cruz, CA). Isoproterenol, MG132, 3-methyladenine (3-MA) and chloroquine (CQ) were purchased from Fisher Scientific (Pittsburgh, PA).

2.2. Cell culture

3T3-L1 preadipocytes were purchased from American Type Culture Collection (Manassas, VA) and maintained in 10% FCS-DMEM in a humidified atmosphere with 5% CO_2 at 37°C. The cells were incubated to differentiate two days post confluency (designated as Day 0) by supplementation of 5 μM DEX, 0.5 mM IBMX, and 167 nM insulin in 10% FBS-DMEM. The medium was changed to 10% FBS-DMEM containing insulin on Day 2 and to 10% FBS-DMEM on Day 4. Cells were differentiated for 8–10 days and subjected to each experiment, as indicated. The brown adipose tissue (BAT) cell line (kindly provided by Prof. Shihuan Kuang, Purdue University) was cultured in DMEM with 10% FBS. The differentiation of BAT cells was induced using a medium containing 2.85 μM insulin, 0.3 μM DEX, 1 μM rosiglitazone, 0.63 mM IBMX, DMEM and 10% FBS for 4 days followed by 4 days of treatment with differentiation medium containing DMEM, 10% FBS, 200 nM insulin and 10 nM triiodothyronine.

2.3. Animal study

All animal treatment was performed under protocol 1112000347, approved by the Purdue Animal Care and Use Committee. Five-week-old male C57BL/6 mice were purchased from Harlan Laboratories (Indianapolis, IN). Mice were maintained on a regular light/dark cycle and kept on a standard chow diet. Six-week-old mice were used for *ex vivo* lipolysis experiments. Three-week-old male C57BL/6J mice purchased from Jackson Laboratories (Bar Harbor, ME) were maintained on a high-fat diet (HFD, 60% of calorie from fat) until 28 weeks of age, at which mice were assigned groups to either HFD + vehicle or HFD + piceatannol (n=8/group). Piceatannol (10 mg/kg body weight) was administered daily via intraperitoneal (*i.p.*) injection for two weeks until euthanasia following overnight fasting. Piceatannol treatment solution was prepared by dissolving in a vehicle solution of 30% polyethylene glycol-400, 1% polysorbate-80, and 1% ethanol. The solution was prepared fresh twice per week and stored at 4°C. At the end of the study, mice were euthanized by asphyxiation using CO_2 and cervical dislocation. Immediately following euthanasia, body composition was analyzed using dual-energy X-ray absorptiometry (DEXA) (PIXImus, Fitchburg, WI). Tissues were weighed and immediately frozen using dry ice and ethanol.

Blood samples were collected from overnight fasted mice through cardio-puncture and stored on ice until centrifugation at 1,500 × g for 10 minutes at 4°C.

2.4. Lipolysis assay

For the *in vitro* lipolysis assay, 3T3-L1 cells and BAT cells were differentiated for 8–10 days and treated as indicated in each experiment. Conditioned media was collected for free glycerol and NEFA measurement. For the *ex vivo* lipolysis assay, C57BL/6 mice were fasted overnight before being sacrificed. Epididymal fat pads were collected, washed in phosphate-buffered saline (PBS), and diced into small pieces. 50 mg of tissue was incubated with piceatannol in DMEM containing 1% fatty acid-free bovine serum albumin (BSA) for 90 min. The medium was collected to measure glycerol and FFA release. Levels of glycerol and FFA were determined using free glycerol reagent (Sigma, St. Louis, MO) and NEFA detection kit (Zen-bio, Research Triangle Park, NC), respectively, following the manufacturer's instructions.

2.5. Immunoblot assay

Differentiated 3T3-L1 cells and isolated mouse adipose tissue were subjected to lysis buffer containing Tris-HCl (100 mM, pH 8.0), NaCl (100 mM), TritonX-100 (0.5% v/v), protease inhibitor cocktail, sodium orthovanadate (1 mM), and sodium fluoride (10 mM) to prepare cell and tissue lysates. Protein concentration was determined by a protein assay kit (Bio-Rad Laboratories, Hercules, CA). Proteins were separated by 10% SDS-polyacrylamide gel electrophoresis, followed by transfer onto nitrocellulose membrane using Mini Trans-Blot electrophoretic transfer cell (Bio-Rad Laboratories, Hercules, CA). After transfer, the membrane was washed and blocked in 5% non-fat milk in Tris-buffered saline with 0.1 % Tween-20 (TBST) for 1 hr at room temperature and probed with the indicated antibodies overnight at 4°C. The immunoblot was visualized with horseradish peroxide-conjugated secondary antibodies and enhanced by chemiluminescence (Thermo Fisher Scientific, Waltham, MA). Western blots were also developed by fluorescent secondary antibodies and imaged by a LI-COR Odyssey CLx imaging system (Licor, Lincoln, NE). Briefly, membranes were blocked by Licor blocking buffer for 1 h, followed by incubation with primary antibodies overnight, washed with PBS, incubated in secondary antibodies for 1 h, washed with PBS, and imaged on the Odyssey Clx. The primary antibodies were described in Materials and Reagents. The secondary antibodies (1:10,000) were produced in goat to the species of the primary antibody and were conjugated with IRdye fluorophores visible in the 700 and 800 channels of the CLx imager. Images were acquired on the CLx imager at 169 μm resolution.

2.6. Immunofluorescence assay

HeLa cells were cultured in cover glass-inserted plates overnight and then treated with the indicated treatments for 2 hrs. The cells were fixed with 3.7% formaldehyde for 30 min and permeabilized in 0.2% Triton-contained PBS for 20 min at room temperature. PBS containing 1% bovine serum albumin and 0.1 % Tween-20 was used for blocking, and the cells were incubated with LC3 antibody (1:100) (Novus Biologicals, Centennial, CO). Primary antibody binding was detected using a Texas red-conjugated secondary antibody (Thermo Fisher Scientific, Waltham, MA). 4′−6-Diamidino-2-phenylindole

(DAPI) (Calbiochem, San Diego, CA) was used for nuclear staining. LC3 and DAPI signals from the cells were visualized by LSM 710 confocal microscopy (Carl Zeiss, Inc., Thornwood, NY).

GFP-expressing *S. Typhimurium* (ATCC, Manassas, VA) were grown following the manufacturer's protocol. To test the protective role of piceatannol in bacteria infection through autophagy, adipocytes (10^5/well) were treated with or without 50 μM piceatannol for 90 min, following the treatment of 5 mM 3-Methyladenine (3-MA, Sigma-Aldrich, Inc., St. Louis, MO) for 24 hrs. In a parallel experiment, adipocytes were treated with either vehicle or Pic in the absence of 3-MA. Cells were then infected with 2×10^7 freshly grown *S. Typhimurium*. At 30-min post infection, cells were washed three times with PBS and incubated in serum-free medium supplemented with 100 μg/ml of Gentamicin for 5 hours to remove extracellular bacteria. Cells were subjected to immunofluorescence assay with α-tubulin antibody (Santa Cruz Biotechnology, Inc., Dallas, TX) and a Texas red-conjugated secondary antibody. α-tubulin and GFP signals from the cells were visualized by LSM 710 confocal microscopy.

2.7. Indirect calorimetry

Mice were transferred to an indirect calorimetry system (Oxymax, Columbus Instruments, Columbus, OH) and individually housed to determine energy expenditure using Weir constants [($VO_2\times3.9$)+($VCO_2\times1.1$)] and respiratory exchange ratio (VCO_2/VO_2). During this time, mice were maintained on a 12-hour light/dark cycle and had free access to food and water. The metabolic chamber detected VO_2 and VCO_2 every 22 minutes.

2.8. Intraperitoneal glucose tolerance test

An intraperitoneal glucose tolerance test (IPGTT) was conducted by first collecting blood from the tail vein of mice after an overnight fast to determine baseline fasting glucose using a glucometer (Bayer Contour, Bayer Healthcare, LLC, Mishawaka, IN). A bolus of 50% glucose solution at 2 g/kg body weight was immediately administered intraperitoneally, and blood glucose was measured at 15, 30, 60, and 120 minutes.

2.9. Serum measurements

Serum insulin and leptin were determined by ELISA following the manufacturer's protocol. Free glycerol and triglycerides were determined spectrophotometrically using the supplier's instructions, where true serum triglycerides were calculated as the difference between total triglycerides (following lipase treatment) and free glycerol (Sigma, St. Louis, MO). Similarly, serum-free cholesterol and cholesterol ester were determined based on the manufacturer's protocol (Biovision Inc., Milpitas, CA). Serum alanine transaminase (Thermo Fisher Scientific, Waltham, MA) and FFA (Sigma, St. Louis, MO) were also determined using the manufacturer's protocol.

2.10. RNA isolation and qPCR

A portion of epididymal white adipose tissue (WAT) was collected in RNAlater at the time of necropsy and stored in TRIzol at −80°C until analysis. Tissue samples were then thawed on ice and homogenized with additional TRIzol to achieve proper

dilution. The total RNA was extracted using the manufacturer's protocol. M-MuLV reverse transcriptase kit was combined with isolated RNA (2 μg/ul) in order to synthesize cDNA. Samples were then amplified by PCR. Diluted cDNA, primers of interest, and SYBR green Taq mixture were combined to analyze mRNA expression using quantitative PCR (qPCR) in the StepOne real-time PCR system (Applied Biosystems, Foster City, CA). *PPARG* forward: CCCAATGGTTGCTGATTACAAT, reverse: CTACTTTGATCGCACTTTGGTATTCT; *FAS* forward: GCCACCCACCGTCAGAAG, reverse: TGTCACATCAGCCACTTGAGTGT; *Leptin* forward: CACACACGCAGTCGGTATCC, reverse: AGCCCAGGAATGAAGTCCAA; *ATGL* forward: GAGACCAAGTGGAACATC, reverse: GTAGATGTGAGTGGCGTT; *CGI-58* forward: TGGTGTCCCACATCTACATCA, reverse: CAGCGTCCATATTCTGTTTCCA; *RPL27* forward: CCTGGCCGGACGCTACT, reverse: AGGTGCCATCGTCAATGTTCT; and *β-actin* forward: AGATGACCCAGATCATGTTTGAGA, reverse: CACAGCCTGGATGGCTACGT. Expression was calculated using the ΔΔCT method using *β-actin* or *RPL27* as the housekeeping gene.

2.11. Statistical analysis

All numerical values are presented as mean ± S.E.M. and data are represented from a minimum of three independent experiments. The statistical analysis of the experimental data was performed by using the software SAS 9.2. A two-tailed Student's t-test was used to determine the statistical difference between the two groups. For the comparisons of multiple means in Fig. 3, a one-way analysis of variance was used, followed by the Dunnett's test to determine the significant difference, with $P < 0.05$ considered significant. Data with different letters are considered statistically different.

3. Results

3.1. Piceatannol inhibits lipolysis by promoting degradation of ATGL, CGI-58 and PLIN1 in adipocytes

To further understand the role of piceatannol in lipid metabolism, we investigated the effect of piceatannol on lipolysis in differentiated 3T3-L1 adipocytes by measuring the release of glycerol and NEFAs from adipocytes. Mature 3T3-L1 adipocytes were treated with various piceatannol concentrations (0 μM −50 μM) in DMEM containing 1% fatty acid-free bovine serum albumin for 90 min in the presence or absence of isoproterenol, a non-selective β-adrenergic agonist. Piceatannol treatment resulted in a dose-dependent inhibition of glycerol and FFA release both at the basal and isoproterenol-stimulated conditions (Fig. 1A, B). Similarly, piceatannol treatment inhibited cAMP-stimulated lipolysis in 3T3-L1 adipocytes when treated with forskolin (Fig. S1A) and IBMX (Fig. S1B). To further verify the inhibitory effect of piceatannol on lipolysis, minced mouse WAT was treated with or without piceatannol in DMEM containing 1% fatty acid-free bovine serum albumin for 90 min and the release of glycerol and NEFAs in the media was measured. Similar to our *in vitro* study, a 90-min piceatannol treatment inhibited the release of glycerol (Fig. S1C) and NEFAs (Fig. S1D) from isolated mouse WAT *ex vivo*, providing evidence to support an anti-lipolytic function of piceatannol.

To gain mechanistic insight into piceatannol-inhibited lipolysis, the effect of piceatannol treatment on the levels of LD-associated lipolytic proteins in adipocytes was examined by immunoblot analysis. We noted that piceatannol treatment resulted in a significant decrease in ATGL, CGI-58 and PLIN1 levels in a dose- (Fig. 1C) and time-dependent manner (Fig. 1D). However, there was no significant effect on the mRNA levels of *ATGL* and *CGI-58* in adipocytes (Fig. S1E). Piceatannol treatment also resulted in a dose-dependent inhibition of glycerol release (Fig. 1E) and suppression of ATGL and PLIN1 levels (Fig. 1F) in cultured brown adipocytes. Collectively, our results indicate a potential non-genomic effect of piceatannol on lowering ATGL, CGI-58, and PLIN1 protein levels in adipocytes.

Resveratrol has been reported to modulate lipolysis, possibly through an increase in Sirt1 activity [21], an inhibition of phosphodiesterase activity [22], and an increase in *ATGL* expression [23]. Since resveratrol shares structural similarity with piceatannol, we next investigated whether resveratrol also displays an anti-lipolytic property in adipocytes. Unlike piceatannol, 90-min of 50 μM resveratrol treatment showed no effect on the release of NEFAs (Fig. 1G) both in basal and isoproterenol-stimulated conditions and ATGL levels (Fig. 1H). Collectively, these results indicate a distinct role of piceatannol in lipolysis as compared with resveratrol, in that piceatannol acutely inhibits lipolysis through suppression of ATGL, CGI-58 and PLIN1 levels in adipocytes.

3.2. Piceatannol promotes autophagy-lysosome pathway-dependent degradation of a lipolytic protein cluster of ATGL, CGI-58, and PLIN1

Our results in Fig. 1 implicate a potential role of piceatannol in the degradation of lipolytic proteins in adipocytes. Since proteasomal proteolysis and the autophagy-lysosome system are primary mechanisms of protein degradation in eukaryotes [24], we first examined the possible role of proteasomal proteolysis in mediating piceatannol-degraded lipolytic proteins in adipocytes using MG132, a proteasome inhibitor. However, MG132 treatment resulted in no effect on piceatannol-induced inhibition of glycerol release in adipocytes (Fig. 2A) or degradation of ATGL (Fig. 2B). We next examined whether the autophagy-lysosome pathway mediated piceatannol-induced degradation of lipolytic proteins by using 3-MA, which inhibits autophagy by blocking type III PI3K activity [25, 26], and the lysosome inhibitor CQ [27]. Consistent with the previous studies [28, 29], both 3-MA and CQ increased glycerol release of adipocytes in the basal condition (Fig. 2C, E). Moreover, piceatannol-suppressed glycerol release was reversed by 3-MA (Fig. 2C) and CQ treatments (Fig. 2E). Notably, a 90-min 3-MA or CQ treatment blunted piceatannol-induced degradation of ATGL, CGI-58 and PLIN1 (Fig. 2D), and ATGL (Fig. 2F) in adipocytes, respectively. These results imply a possibility of an autophagy-dependent piceatannol-promoted degradation of lipolytic proteins in adipocytes. Upon autophagy activation, the autophagy protein LC3 (microtubule-associated protein 1 light chain 3α) becomes conjugated to phosphatidylethanolamine (PE) to form lipid-conjugated LC3 (LC3-II) located on the membrane of the autophagosomes [30]. Indeed, our immunofluorescence analysis revealed an increased LC3 expression and punctuated distribution of LC3 in HeLa cells treated with piceatannol both in the presence or absence of 3-MA (Fig. 3A). We also observed that acute piceatannol treatment altered expression of autophagy marker proteins in adipocytes, as evidenced by an increase of autophagy-related gene 7 (ATG7) and a

decrease of autophagosome cargo p62 levels. The effect of piceatannol on ATG7 and p62 was alleviated in adipocytes when treated with 3-MA (Fig. 3B). As autophagy is known to be a defensive degradation mechanism against intracellular pathogen infection [31] such as the food-borne pathogen *S. typhimurium* [32, 33], we further tested whether piceatannol-induced autophagy could protect adipocytes from infection by *S. typhimurium.* We found that 3T3-L1 adipocytes were resistant to S. typhimurium infection regardless of the presence of piceatannol as shown by little or no signal of GFP-expressing *S. typhimurium* after 30-min of bacterial infection (Fig. 3C top left vs. top right). This resistance to *S. typhimurium* infection was diminished when the basal autophagy in 3T3-L1 adipocytes was impaired by 3-MA treatment as demonstrated by an approximately 6-fold increase in the GFP signal in 3T3-L1 adipocytes. However, piceatannol treatment resulted in a reversal of 3-MA-attenuated basal autophagy in 3T3-L1 adipocytes as demonstrated by a lower intracellular GFP signal in 3-MA and piceatannol co-treated adipocytes than that of 3-MA-treated cells. These results indicate that piceatannol protects 3T3-L1 adipocytes from 3-MA-promoted *S. typhimurium* infection. These results strongly support the role of piceatannol in autophagy activation in adipocytes.

3.3. Piceatannol administration lowers lipolysis, obesity-associated central adiposity and hyperinsulinemia *in vivo*

In order to verify the anti-lipolytic potential of piceatannol *in vivo*, overnight fasted wild-type obese C57BL/6 mice were subjected to an intraperitoneal (*i.p.*) injection of piceatannol (10 mg/kg body weight) or vehicle solution. After 8 h of piceatannol administration, mice were sacrificed to determine the effect of piceatannol on fasting-induced lipolysis. Piceatannol administration showed no effect on fasting-decreased serum glucose levels (Fig. 4A). Although not statistically significant ($p = 0.074$), piceatannol treatment tended to inhibit lipolysis, as judged by a reduction in fasting-induced serum glycerol levels after piceatannol treatment (Fig. 4B).

To investigate the functional impact of piceatannol on obesity-associated lipolysis *in vivo,* 6-week-old male C57BL/6 mice were fed a high-fat diet (HFD) for 24 weeks followed by daily *i.p.* injection of vehicle or piceatannol (10 mg/kg/day) for 15 days. The mice in both groups showed no apparent alteration in body weight (Fig. 4C) at the end of the study. In contrast, piceatannol administration slightly decreased food intake (Fig. 4D) and epididymal white adipose tissue weight (Fig. 4E), and tended to decrease total body fat content ($p = 0.056$, Fig. 4F). To assess piceatannol's effect on energy homeostasis, we monitored the metabolic parameters of piceatannol-treated mice by indirect calorimetry. There was no noticeable difference in energy expenditure in both the light and dark cycles between the two groups (Fig. 4G), suggesting similar basal metabolism. The lack of available physical activity data limits conclusions regarding other effects of piceatannol on overall energy expenditure. However, piceatannol-treated mice had a lower respiratory exchange ratio (RER) than vehicle-treated mice (Fig. 4H), indicating a shift in substrate utilization towards enhanced lipid oxidation in the piceatannol-treated mice.

No differences in the levels of serum alanine transaminase, an indicator of liver injury, (Fig. 5A), serum glucose (Fig. 5B), and glucose tolerance (Fig. 5C) were detected between

the two groups of mice. Notably, piceatannol treatment lowered serum insulin levels (Fig. 5D). Consistent with our *in vitro* results and the acute suppressive effect of piceatannol in fasting-induced serum glycerol levels (Fig. 4B), a 15-day piceatannol administration resulted in approximately 25 % and 33 % decreases in serum-free fatty acids (Fig. 5E) and glycerol (Fig. 5F) levels, respectively, in obese mice. Moreover, piceatannol-administrated mice exhibited a 38 % lower serum leptin level compared with control mice (Fig. 5G). However, there were no differences in serum lipid levels such as TG, free cholesterol, and cholesterol ester (Fig, 5H–J) between the two groups of mice.

We next tested whether piceatannol-suppressed serum markers of lipolysis are associated with changes in the protein levels of ATGL and CGI-58 in adipose tissue. The WAT isolated from mice treated with vehicle and piceatannol displayed decreased protein levels of ATGL with no noticeable change in CGI-58 levels (Fig. 6A and B). Furthermore, piceatannol showed no effect on the mRNA levels of adipocyte marker genes such as *PPARG* and *FAS*, and the genes involved in lipolysis such as *ATGL* and *CGI-58* (Fig. 6C). Consistent with the reduced epididymal fat pad weight in Fig. 4E and the serum level of leptin in piceatannol-treated mice in Fig. 5G, these mice displayed a significantly lower levels of *leptin* mRNA in epididymal WAT compared with control vehicle-treated mice (Fig. 6C).

4. Discussion

In the present study, we highlight a new role of piceatannol in impeding adipocyte lipolysis through degradation of the key lipolytic proteins. We further provide direct evidence that activation of the autophagy-lysosome pathway is required to mediate piceatannol-induced degradation of lipolytic proteins in adipocytes, thereby impacting obesity-related lipolysis.

Elevated plasma NEFA levels and overly activated adipose lipolysis are reported to exacerbate obesity-related insulin resistance and hepatic dysfunction primarily through the lipotoxic potential of FAs in the peripheral tissues [1, 2]. Accordingly, partial inhibition of lipolysis is proposed as an attractive approach to lower plasma NEFA levels and their associated lipotoxicity. This notion has been partly supported by evidence from studies of various animal models lacking the *ATGL* [34], *HSL* [14], or *MAGL* [35] gene, or employing a small-molecular inhibitor for HSL [14] or ATGL [13]. However, safe therapeutics that inhibit lipolysis by targeting multiple lipolytic proteins have yet to be explored.

Our current study fills this gap by identifying piceatannol as a natural small molecule inhibitor of lipolysis. Indeed, the anti-lipolytic property of piceatannol was previously proposed by Les et al. [36] in that piceatannol exhibited an anti-lipolytic effect in adipocytes *in vitro,* mostly at physiologically irrelevant doses. Our study further demonstrates that piceatannol suppressed glycerol and FA release from differentiated adipocytes and brown adipocytes both at basal and stimulated lipolysis conditions at lower does ranging 25 μM – 50 μM *in vitro*. Although limited data are currently available regarding the physiological doses of piceatannol and its bioavailability in humans, a single intravenous administration of piceatannol (10 mg/kg) in rats showed C_{max} of piceatannol at 41 μM in 6hr [37]. Furthermore, our study demonstrates that intraperitoneal administration of piceatannol at 10 mg/kg BW appeared to suppress fasting-induced plasma glycerol levels in mice

(Fig. 4B). These results support that 10 mg/kg BW of piceatannol could be applicable to physiological conditions and affect energy metabolism. Furthermore, we showed that piceatannol administration lowered fasting-induced plasma glycerol both in lean and obese mice. Notably, a 15-day treatment of piceatannol rendered a decrease in visceral adipose tissue mass and plasma levels of FFAs, glycerol, insulin, and leptin, and shifted substrate utilization towards lipid oxidation in diet-induced obese mice. Despite its anti-lipolytic function, piceatannol-treated diet-induced obese mice did not display systemic accumulation of TG in peripheral tissues such as WAT and the liver, as reported in the mice with genetic inactivation of lipolysis [38]. Piceatannol administration rather resulted in a decrease in epididymal fat pad weight in diet-induced obese mice. Our finding of lower WAT weight is in accordance with previous studies showing that pharmacological inhibition of lipolysis lowers TG accumulation in WAT both in lean [39] and high-fat diet-induced animals [12, 13]. The apparently opposing observations of lipolysis inhibition and epididymal fat pad weight reduction is likely explained by piceatannol's effect on other lipid-related pathways. For example, piceatannol is known to inhibit lipogenesis and TG accumulation, modulate the gut microbiota profile, and increase fatty acid oxidation *in vivo*[40]. Our observation of increased RER in piceatannol-treated mice suggest the piceatannol may also alter fatty-acid oxidation. Further studies investigating the mechanism by which piceatannol may reduce WAT mass are merited.

The most intriguing finding of this study was the acute and robust effect of piceatannol on the degradation of lipolytic proteins that are needed for LD catabolism. Acute piceatannol treatment led to a marked reduction of ATGL, CGI-58, and PLIN1 levels in adipocytes with little effect on HSL levels. Despite the fact that more than 50 % of piceatannol is degraded in the cell culture media in about 12 hr (Kershaw, J. *et al.* unpublished data), the levels of piceatannol-degraded lipolytic protein clusters remained low after 24 hr of treatment. This warrants a more detailed study of the degradation kinetics of lipolytic protein clusters in piceatannol-treated adipocytes. To elucidate the potential mechanism underlying piceatannol-induced degradation of the lipolytic protein cluster in adipocytes, we probed the autophagy-lysosome-dependent protein degradation pathway. Using various autophagy and lysosome inhibitors, we found that piceatannol-induced degradation of the lipolytic protein clusters in adipocytes requires activation of the autophagy-lysosome system, indicating a pro-autophagic effect of piceatannol in adipocytes. In addition to cytosolic LD breakdown, the activation of autophagy is suggested to participate in LD catabolism both in basal and nutrient-deficient conditions through activation of lipophagy-, autophagy-induced selective sequestration of LD to the autophagosome and the resulting degradation of lipids by lysosomal lipases [41]. This selective targeting of LD to autophagosomes requires recognition of LD-associated proteins and their autophagic degradation in various cells, including adipocytes. For example, chaperon-mediated autophagy (CMA)-induced degradation of LD-associated PLINs is shown to be necessary for LD lipophagy [42, 43]. Consistently, our finding of piceatannol-induced PLIN1 degradation in adipocytes supports a potential causative role of piceatannol in lipophagy induction. On the other hand, the current understanding of ATGL's role in adipocyte lipophagy is largely limited to the ability of autophagy-lysosome-dependent enzymatic LD breakdown [44] and an upstream regulator of lipophagy [45]. However, the direct targeting of ATGL to autophagy-dependent degradation

has not yet been reported. Our study provides the first investigation, to our knowledge, of an autophagy-induced selective degradation of ATGL and an ATGL-interacting coactivator CGI-58 by piceatannol, a natural polyphenol, in adipocytes. We demonstrated that acute treatment of cultured adipocytes and brown adipocytes with piceatannol resulted in the degradation of ATGL, CGI-58, and PLIN1. Importantly, chemical inhibition of autophagy and lysosome activity blocked the effect of piceatannol on the degradation of these proteins. Notably, previous studies suggest that piceatannol's action in autophagy appears to be cell-type specific. Piceatannol was shown to promote autophagy in human leukemia cells [46], fibrosarcoma cells [47], and osteosarcoma cells [48], as judged by p62 degradation and LC3 lipidation. Contrary to these studies, piceatannol inhibited methylglyoxal-induced autophagy in murine osteoblastic cells [49] and oxidized low-density lipoprotein-induced autophagy in bone marrow-derived macrophages [50]. Unlike piceatannol, other known autophagy activators such as PP242 (a mTORC2 specific inhibitor) and trehalose (a transcription factor EB inducer) failed to inhibit forskolin-stimulated lipolysis in adipocytes (Kershaw, J. *et al*. unpublished data). Collectively, our results reveal piceatannol as potential novel food-derived regulator of adipocyte lipolysis through autophagy-induced selective degradation of lipolytic proteins. In order to elucidate the mechanism by which piceatannol induces selective degradation of lipolytic protein clusters, future endeavors need to resolve the following issues: investigation of (i) piceatannol-induced recognition of these proteins to autophagy components; and (ii) piceatannol-induced selective recruitment of these proteins to lysosomal degradation in adipocytes.

In conclusion, our study provides profound evidence of a novel function of piceatannol in modulating lipolysis and promoting autophagy-lysosome-dependent degradation of the key lipolytic proteins in adipocytes. This study provides a mechanistic foundation to investigate piceatannol-containing foods as a possible dietary strategy to reduce lipolysis and fatty acid-induced lipotoxicity, thereby lowering lipotoxicity-related metabolic disorders.

Supplementary Material

Refer to Web version on PubMed Central for supplementary material.

Funding sources

This work was supported, in part, by a grant from the National Institutes of Health (5R03CA184544, KHK), the USDA National Institute of Food and Agriculture Hatch project (1013613, KHK), and a USDA National Needs Fellowship program (2012-38420-30207, JK).

Abbreviations:

ABHD5	α/β hydrolase domain-containing 5
ATGL	adipose triglyceride lipase
DG	diacylglycerol
CGI-58	comparative gene identification-58
FoxO1	forkhead box protein O1

HSL	hormone-sensitive lipase
LDs	lipid droplets
MAG	monoacylglycerol
MAGL	MAG lipase
NEFAs	non-esterified fatty acids
NF-κB	nuclear factor-κB
PI3K	phosphoinositide 3-kinase
PLIN1	perilipin1
PNPLA2	patatin-like phospholipase domain-containing protein 2
PKA	protein kinase A
PPARγ	peroxisome proliferator-activated receptorγ
SYK	spleen tyrosine kinase
TG	triacylglycerol

References

[1]. Boden G Role of fatty acids in the pathogenesis of insulin resistance and NIDDM. Diabetes. 1997;46:3–10. [PubMed: 8971073]

[2]. Czech MP. Insulin action and resistance in obesity and type 2 diabetes. Nat Med. 2017;23:804–14. [PubMed: 28697184]

[3]. Zimmermann R, Strauss JG, Haemmerle G, Schoiswohl G, Birner-Gruenberger R, Riederer M, et al. Fat mobilization in adipose tissue is promoted by adipose triglyceride lipase. Science. 2004;306:1383–6. [PubMed: 15550674]

[4]. Villena JA, Roy S, Sarkadi-Nagy E, Kim KH, Sul HS. Desnutrin, an adipocyte gene encoding a novel patatin domain-containing protein, is induced by fasting and glucocorticoids: ectopic expression of desnutrin increases triglyceride hydrolysis. J Biol Chem. 2004;279:47066–75. [PubMed: 15337759]

[5]. Jenkins CM, Mancuso DJ, Yan W, Sims HF, Gibson B, Gross RW. Identification, cloning, expression, and purification of three novel human calcium-independent phospholipase A2 family members possessing triacylglycerol lipase and acylglycerol transacylase activities. J Biol Chem. 2004;279:48968–75. [PubMed: 15364929]

[6]. Lefevre C, Jobard F, Caux F, Bouadjar B, Karaduman A, Heilig R, et al. Mutations in CGI-58, the gene encoding a new protein of the esterase/lipase/thioesterase subfamily, in Chanarin-Dorfman syndrome. Am J Hum Genet. 2001;69:1002–12. [PubMed: 11590543]

[7]. Lass A, Zimmermann R, Haemmerle G, Riederer M, Schoiswohl G, Schweiger M, et al. Adipose triglyceride lipase-mediated lipolysis of cellular fat stores is activated by CGI-58 and defective in Chanarin-Dorfman Syndrome. Cell Metab. 2006;3:309–19. [PubMed: 16679289]

[8]. Ahmadian M, Duncan RE, Varady KA, Frasson D, Hellerstein MK, Birkenfeld AL, et al. Adipose overexpression of desnutrin promotes fatty acid use and attenuates diet-induced obesity. Diabetes. 2009;58:855–66. [PubMed: 19136649]

[9]. Hoy AJ, Bruce CR, Turpin SM, Morris AJ, Febbraio MA, Watt MJ. Adipose triglyceride lipase-null mice are resistant to high-fat diet-induced insulin resistance despite reduced

energy expenditure and ectopic lipid accumulation. Endocrinology. 2011;152:48–58. [PubMed: 21106876]

[10]. Ahmadian M, Abbott MJ, Tang T, Hudak CS, Kim Y, Bruss M, et al. Desnutrin/ATGL is regulated by AMPK and is required for a brown adipose phenotype. Cell Metab. 2011;13:739–48. [PubMed: 21641555]

[11]. Tang T, Abbott MJ, Ahmadian M, Lopes AB, Wang Y, Sul HS. Desnutrin/ATGL activates PPARdelta to promote mitochondrial function for insulin secretion in islet beta cells. Cell Metab. 2013;18:883–95. [PubMed: 24268737]

[12]. Mayer N, Schweiger M, Romauch M, Grabner GF, Eichmann TO, Fuchs E, et al. Development of small-molecule inhibitors targeting adipose triglyceride lipase. Nat Chem Biol. 2013;9:785–7. [PubMed: 24096302]

[13]. Schweiger M, Romauch M, Schreiber R, Grabner GF, Hutter S, Kotzbeck P, et al. Pharmacological inhibition of adipose triglyceride lipase corrects high-fat diet-induced insulin resistance and hepatosteatosis in mice. Nat Commun. 2017;8:14859. [PubMed: 28327588]

[14]. Girousse A, Tavernier G, Valle C, Moro C, Mejhert N, Dinel AL, et al. Partial inhibition of adipose tissue lipolysis improves glucose metabolism and insulin sensitivity without alteration of fat mass. PLoS Biol. 2013;11:e1001485. [PubMed: 23431266]

[15]. Mongioi LM, La Vignera S, Cannarella R, Cimino L, Compagnone M, Condorelli RA, et al. The Role of Resveratrol Administration in Human Obesity. Int J Mol Sci. 2021;22. [PubMed: 35008458]

[16]. Springer M, Moco S. Resveratrol and Its Human Metabolites-Effects on Metabolic Health and Obesity. Nutrients. 2019;11.

[17]. Kershaw J, Kim KH. The Therapeutic Potential of Piceatannol, a Natural Stilbene, in Metabolic Diseases: A Review. J Med Food. 2017;20:427–38. [PubMed: 28387565]

[18]. Kwon JY, Seo SG, Heo YS, Yue S, Cheng JX, Lee KW, et al. Piceatannol, natural polyphenolic stilbene, inhibits adipogenesis via modulation of mitotic clonal expansion and insulin receptor-dependent insulin signaling in early phase of differentiation. J Biol Chem. 2012;287:11566–78. [PubMed: 22298784]

[19]. Shen P, Yue Y, Kim KH, Park Y. Piceatannol Reduces Fat Accumulation in Caenorhabditis elegans. J Med Food. 2017;20:887–94. [PubMed: 28514198]

[20]. Shen P, Yue Y, Sun Q, Kasireddy N, Kim KH, Park Y. Piceatannol extends the lifespan of Caenorhabditis elegans via DAF-16. Biofactors. 2017;43:379–87. [PubMed: 28128482]

[21]. Picard F, Kurtev M, Chung N, Topark-Ngarm A, Senawong T, Machado De Oliveira R, et al. Sirt1 promotes fat mobilization in white adipocytes by repressing PPAR-gamma. Nature. 2004;429:771–6. [PubMed: 15175761]

[22]. Park SJ, Ahmad F, Philp A, Baar K, Williams T, Luo H, et al. Resveratrol ameliorates aging-related metabolic phenotypes by inhibiting cAMP phosphodiesterases. Cell. 2012;148:421–33. [PubMed: 22304913]

[23]. Lasa A, Schweiger M, Kotzbeck P, Churruca I, Simon E, Zechner R, et al. Resveratrol regulates lipolysis via adipose triglyceride lipase. J Nutr Biochem. 2012;23:379–84. [PubMed: 21543206]

[24]. Dikic I Proteasomal and Autophagic Degradation Systems. Annu Rev Biochem. 2017;86:193–224. [PubMed: 28460188]

[25]. Seglen PO, Gordon PB. 3-Methyladenine: specific inhibitor of autophagic/lysosomal protein degradation in isolated rat hepatocytes. Proc Natl Acad Sci U S A. 1982;79:1889–92. [PubMed: 6952238]

[26]. Blommaart EF, Krause U, Schellens JP, Vreeling-Sindelarova H, Meijer AJ. The phosphatidylinositol 3-kinase inhibitors wortmannin and LY294002 inhibit autophagy in isolated rat hepatocytes. Eur J Biochem. 1997;243:240–6. [PubMed: 9030745]

[27]. Solomon VR, Lee H. Chloroquine and its analogs: a new promise of an old drug for effective and safe cancer therapies. Eur J Pharmacol. 2009;625:220–33. [PubMed: 19836374]

[28]. Heckmann BL, Yang X, Zhang X, Liu J. The autophagic inhibitor 3-methyladenine potently stimulates PKA-dependent lipolysis in adipocytes. Br J Pharmacol. 2013;168:163–71. [PubMed: 22817685]

[29]. Severson DL, Lefebvre FA, Sloan SK. Effect of chloroquine on rates of lipolysis in the isolated perfused rat heart and in rat epididymal fat pads. J Mol Cell Cardiol. 1980;12:977–92. [PubMed: 7463488]

[30]. Bento CF, Renna M, Ghislat G, Puri C, Ashkenazi A, Vicinanza M, et al. Mammalian Autophagy: How Does It Work? Annu Rev Biochem. 2016;85:685–713. [PubMed: 26865532]

[31]. Levine B, Deretic V. Unveiling the roles of autophagy in innate and adaptive immunity. Nat Rev Immunol. 2007;7:767–77. [PubMed: 17767194]

[32]. Hernandez LD, Pypaert M, Flavell RA, Galan JE. A Salmonella protein causes macrophage cell death by inducing autophagy. J Cell Biol. 2003;163:1123–31. [PubMed: 14662750]

[33]. Jia K, Thomas C, Akbar M, Sun Q, Adams-Huet B, Gilpin C, et al. Autophagy genes protect against Salmonella typhimurium infection and mediate insulin signaling-regulated pathogen resistance. Proc Natl Acad Sci U S A. 2009;106:14564–9. [PubMed: 19667176]

[34]. Schoiswohl G, Stefanovic-Racic M, Menke MN, Wills RC, Surlow BA, Basantani MK, et al. Impact of Reduced ATGL-Mediated Adipocyte Lipolysis on Obesity-Associated Insulin Resistance and Inflammation in Male Mice. Endocrinology. 2015;156:3610–24. [PubMed: 26196542]

[35]. Taschler U, Radner FP, Heier C, Schreiber R, Schweiger M, Schoiswohl G, et al. Monoglyceride lipase deficiency in mice impairs lipolysis and attenuates diet-induced insulin resistance. J Biol Chem. 2011;286:17467–77. [PubMed: 21454566]

[36]. Les F, Deleruyelle S, Cassagnes LE, Boutin JA, Balogh B, Arbones-Mainar JM, et al. Piceatannol and resveratrol share inhibitory effects on hydrogen peroxide release, monoamine oxidase and lipogenic activities in adipose tissue, but differ in their antilipolytic properties. Chem Biol Interact. 2016;258:115–25. [PubMed: 27475863]

[37]. Roupe KA, Yanez JA, Teng XW, Davies NM. Pharmacokinetics of selected stilbenes: rhapontigenin, piceatannol and pinosylvin in rats. J Pharm Pharmacol. 2006;58:1443–50. [PubMed: 17132206]

[38]. Radner FP, Streith IE, Schoiswohl G, Schweiger M, Kumari M, Eichmann TO, et al. Growth retardation, impaired triacylglycerol catabolism, hepatic steatosis, and lethal skin barrier defect in mice lacking comparative gene identification-58 (CGI-58). J Biol Chem. 2010;285:7300–11. [PubMed: 20023287]

[39]. Takahara S, Ferdaoussi M, Srnic N, Maayah ZH, Soni S, Migglautsch AK, et al. Inhibition of ATGL in adipose tissue ameliorates isoproterenol-induced cardiac remodeling by reducing adipose tissue inflammation. Am J Physiol Heart Circ Physiol. 2021;320:H432–H46. [PubMed: 33185110]

[40]. Tung YC, Lin YH, Chen HJ, Chou SC, Cheng AC, Kalyanam N, et al. Piceatannol Exerts Anti-Obesity Effects in C57BL/6 Mice through Modulating Adipogenic Proteins and Gut Microbiota. Molecules. 2016;21.

[41]. Cingolani F, Czaja MJ. Regulation and Functions of Autophagic Lipolysis. Trends Endocrinol Metab. 2016;27:696–705. [PubMed: 27365163]

[42]. Kaushik S, Cuervo AM. Degradation of lipid droplet-associated proteins by chaperone-mediated autophagy facilitates lipolysis. Nat Cell Biol. 2015;17:759–70. [PubMed: 25961502]

[43]. Kaushik S, Cuervo AM. AMPK-dependent phosphorylation of lipid droplet protein PLIN2 triggers its degradation by CMA. Autophagy. 2016;12:432–8. [PubMed: 26902588]

[44]. Martinez-Lopez N, Garcia-Macia M, Sahu S, Athonvarangkul D, Liebling E, Merlo P, et al. Autophagy in the CNS and Periphery Coordinate Lipophagy and Lipolysis in the Brown Adipose Tissue and Liver. Cell Metab. 2016;23:113–27. [PubMed: 26698918]

[45]. Sathyanarayan A, Mashek MT, Mashek DG. ATGL Promotes Autophagy/Lipophagy via SIRT1 to Control Hepatic Lipid Droplet Catabolism. Cell Rep. 2017;19:1–9. [PubMed: 28380348]

[46]. Siedlecka-Kroplewska K, Slebioda T, Kmiec Z. Induction of autophagy, apoptosis and aquisition of resistance in response to piceatannol toxicity in MOLT-4 human leukemia cells. Toxicol In Vitro. 2019;59:12–25. [PubMed: 30940561]

[47]. Pietrocola F, Marino G, Lissa D, Vacchelli E, Malik SA, Niso-Santano M, et al. Pro-autophagic polyphenols reduce the acetylation of cytoplasmic proteins. Cell Cycle. 2012;11:3851–60. [PubMed: 23070521]

[48]. Papandreou I, Verras M, McNeil B, Koong AC, Denko NC. Plant stilbenes induce endoplasmic reticulum stress and their anti-cancer activity can be enhanced by inhibitors of autophagy. Exp Cell Res. 2015;339:147–53. [PubMed: 26477823]

[49]. Suh KS, Chon S, Choi EM. Protective effects of piceatannol on methylglyoxal-induced cytotoxicity in MC3T3-E1 osteoblastic cells. Free Radic Res. 2018;52:712–23. [PubMed: 29792365]

[50]. Choi SH, Gonen A, Diehl CJ, Kim J, Almazan F, Witztum JL, et al. SYK regulates macrophage MHC-II expression via activation of autophagy in response to oxidized LDL. Autophagy. 2015;11:785–95. [PubMed: 25946330]

Highlights

- Piceatannol inhibits lipolysis in adipocytes with a concomitant reduction of the lipolytic proteins.
- Piceatannol-inhibited lipolysis resultes from autophagy-lysosome-dependent degradation of the lipolytic proteins in adipocytes.
- Piceatannol administration lowers lipolysis, central adiposity and hyperinsulinemia in diet-induced obese mice

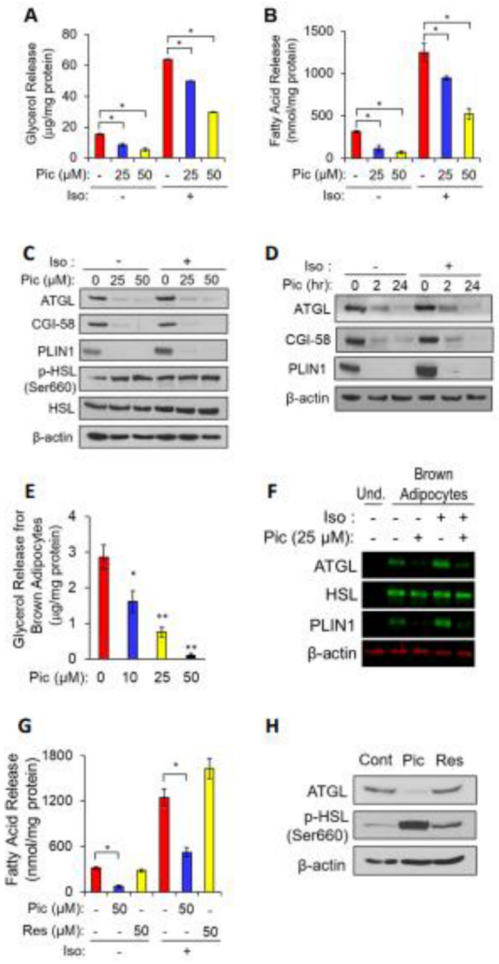

Fig. 1. Piceatannol inhibits lipolysis by lowering ATGL, CGI-58 and PLIN1 levels in adipocytes

Differentiated 3T3-L1 adipocytes (A-D, G, H) and murine brown adipocytes (E.F) were incubated with piceatannol (0–50 μM) or resveratrol (0–50 μM) in the presence or absence of isoproterenol (10 μM) in DMEM containing 1% fatty acid-free bovine serum albumin for 90 min or at the indicated time points. The medium was collected to measure the released glycerol (A, E) and FFA (B, G) levels as described in the Experimental Section. Data are presented as means ± SEM. (n=3, *, $p < 0.05$; **, $p < 0.01$). Total cellular proteins at 90 min or the indicated time points were extracted from the differentiated 3T3-L1 adipocytes (C, D, H) and brown adipocytes (F), and analyzed by Western blot analysis for ATGL, CGI-58, PLIN1, p-HSL, HSL and β-actin. *iso*: isoproterenol, *Pic*: piceatannol, *Res*: resveratrol, *Cont*: control, *Und*: undifferentiated.

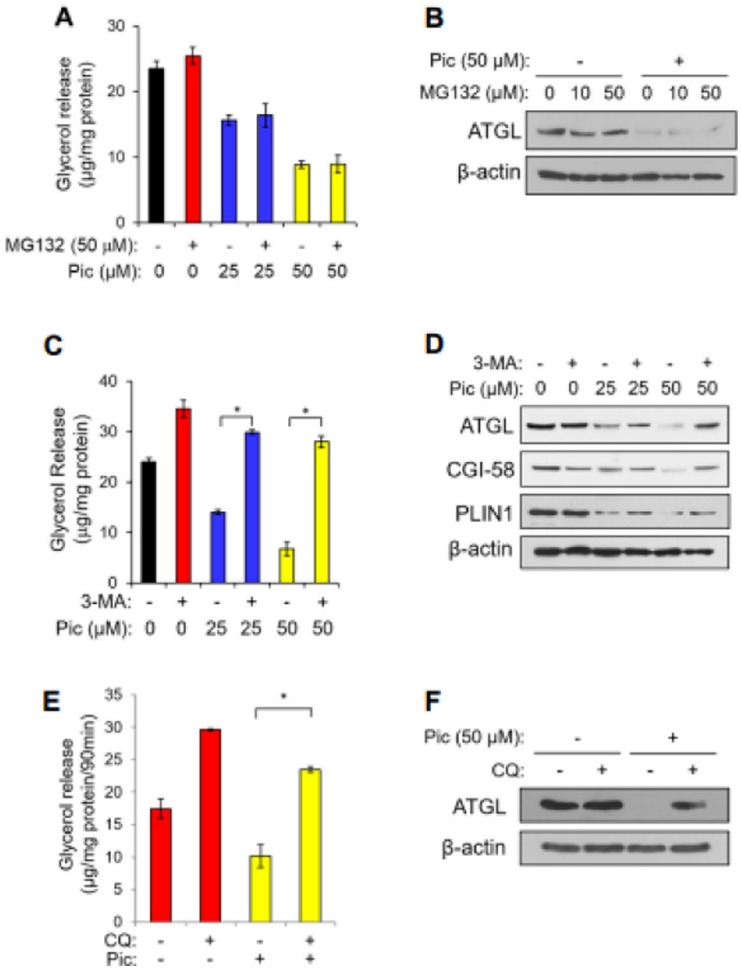

Fig. 2. Piceatannol promotes autophagy-lysosome pathway-dependent degradation of a lipolytic protein cluster of ATGL, CGI-58, and PLIN1 in adipocytes

Differentiated 3T3-L1 adipocytes were incubated with piceatannol (0–50 μM) in the presence or absence of various concentration of MG132 (A, B), 10 mM 3-MA (C, D) and 10 μM CQ (E, F) in DMEM containing 1% fatty acid-free bovine serum albumin for 90 min. The medium was collected to measure the released glycerol (A, C, E) levels as described in the Experimental Section. Data are presented as means ± SEM. (n=3, *, $p < 0.05$). Total cellular proteins isolated from these cells were analyzed by Western blot analysis for ATGL, CGI-58, PLIN1 and β-actin (B, D, F).

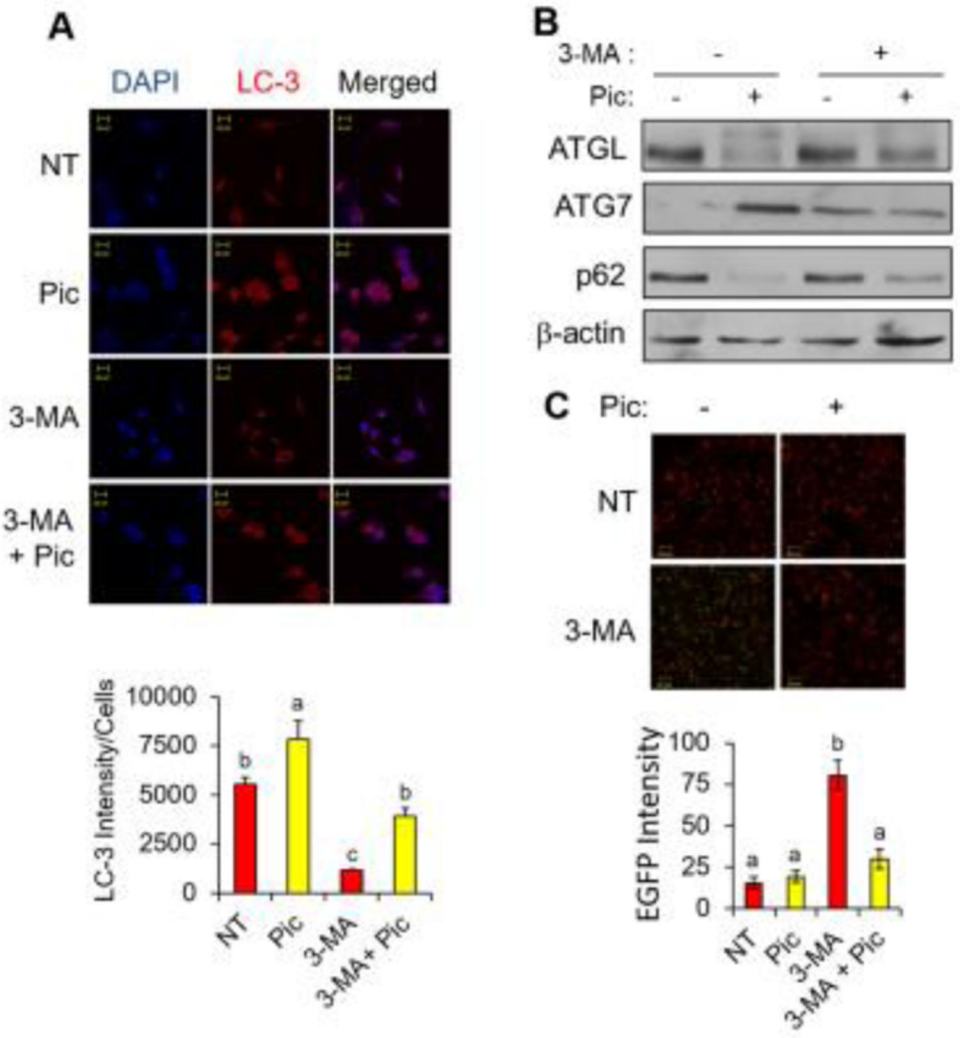

Fig. 3. Piceatannol treatment stimulates autophagy *in vitro*.

(A) Immunofluorescence analysis of Hela cells treated with 50 μM piceatannol (*Pic*), 5 mM 3-MA or the combination of Pic and 3-MA in serum-free medium for 2 hr (LC3: red and DAPI: blue) (top). Quantification of the fluorescence intensity of LC3 was shown (bottom). **(B)** Hela cells described in panel A were then subjected to Western blot analysis for ATGL, ATG7, p62 and β-actin. **(C)** 3T3-L1 adipocytes were treated with piceatannol (25 μM) for 90 min followed by GFP-expressing *S. typhimurium* infection for 30 min. α-tubulin (red) and EGFP (green) signals were visualized by confocal microscopy (top). Quantification of the fluorescence intensity of EGFP was shown (bottom). Scale bar indicates 20 μm. Data are presented as means ± SEM and different letters indicate statistical significance. *NT*: non-treated.

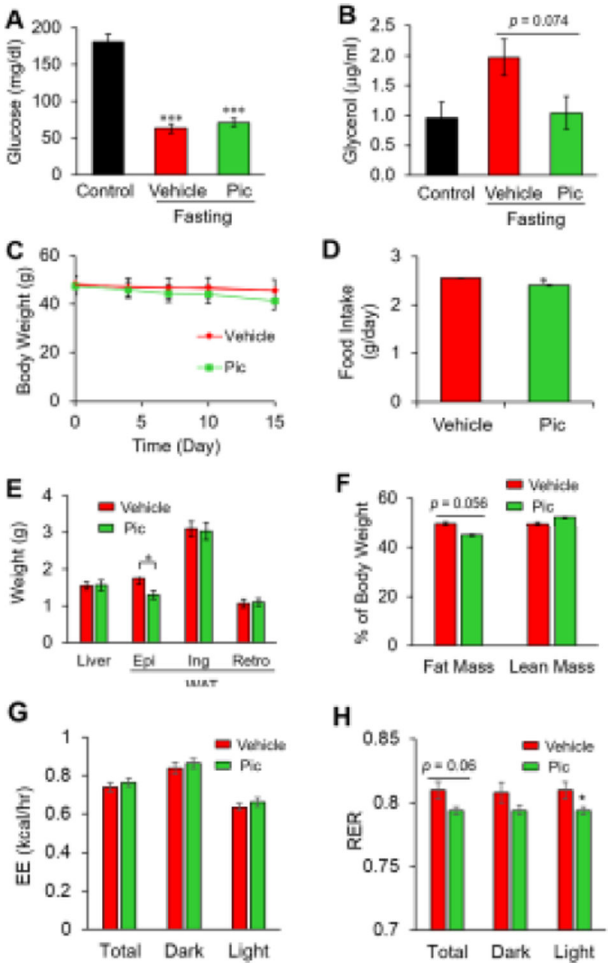

Fig. 4. Piceatannol administration suppresses fasting-induced serum glycerol and obesity-associated central adiposity *in vivo*.

Overnight fasted wild-type obese C57BL/6J mice (n=3/group) were subjected to *i.p.* injection of piceatannol (10 mg/kg body weight) or vehicle solution for 8 h followed by serum glucose (**A**) and glycerol (**B**) analyses. Diet-induced obese mice (n=6–8/group) were administered (10 mg/kg body weight) via *i.p.* injection for 15 days. Body weight (**C**) and food intake (**D**) were measured during the study. Weight of liver and WAT (*Epi*: epididymal, *Ing*: inguinal, *Ret*: retroperitoneal) (**E**) and percent fat mas and lean mass (**F**) were measured at the end of the study. After 14-days of piceatannol administration, mice were put into a metabolic chamber to measure energy expenditure (EE) (**G**) and respiratory exchange ratio (RER) (**H**). Data are presented as means ± SEM. (*, $p < 0.05$).

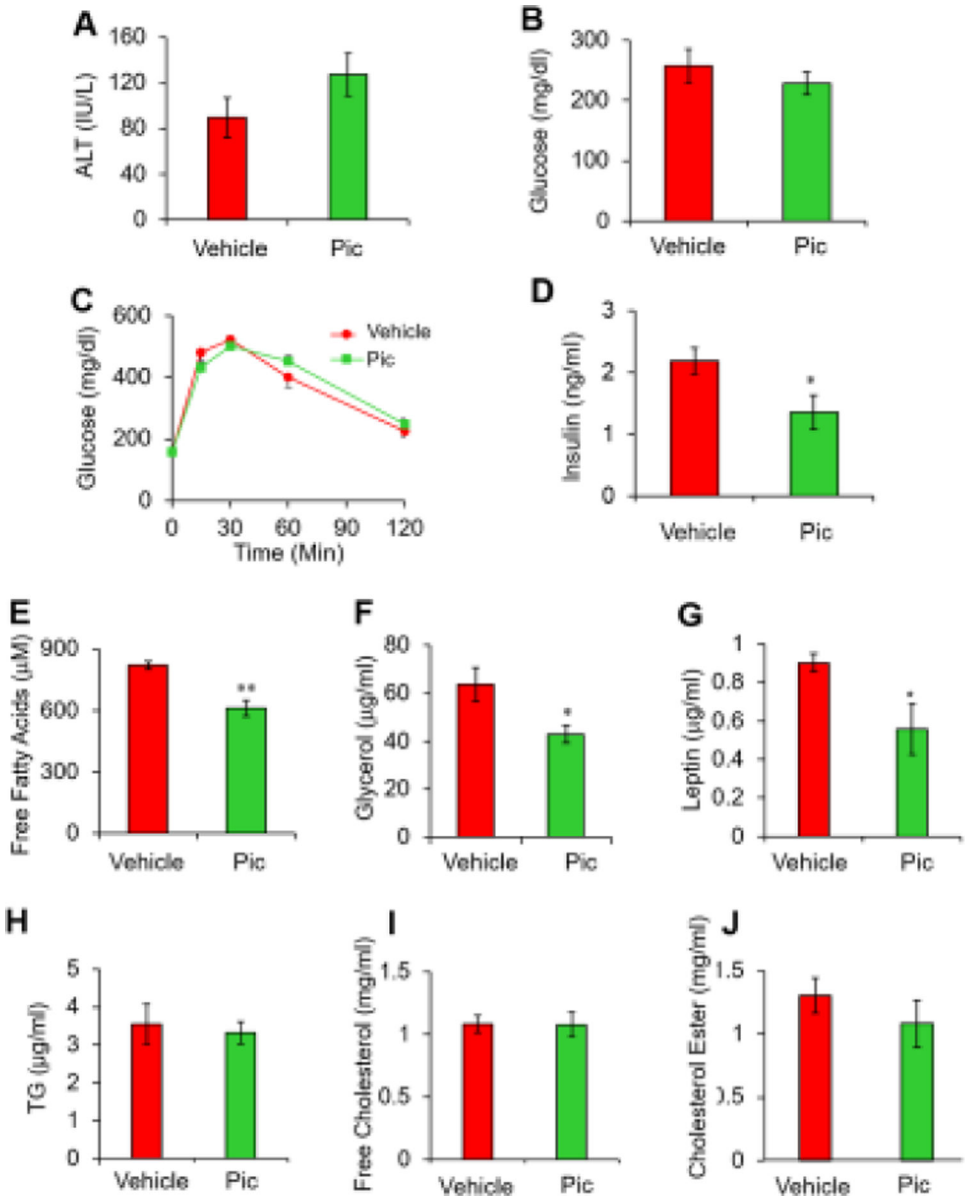

Fig. 5. Piceatannol administration improves serum levels of insulin, free fatty acids, glycerol and leptin in diet-induced obese mice.

Serum levels of alanine transaminase (**A**), glucose (**B**), insulin (**D**), free fatty acids (**E**), glycerol (**F**), leptin (**G**), TG (**H**), free cholesterol (**I**) and cholesterol ester (**J**) were measured in overnight-fasted piceatannol-treated diet-induced obese mice. (**C**) An IPGTT was performed in mice with 2 g/kg glucose *i.p.* injection at the end of the study. Data are presented as means ± SEM. (n=7–8, *, $p < 0.05$; **, $p < 0.01$).

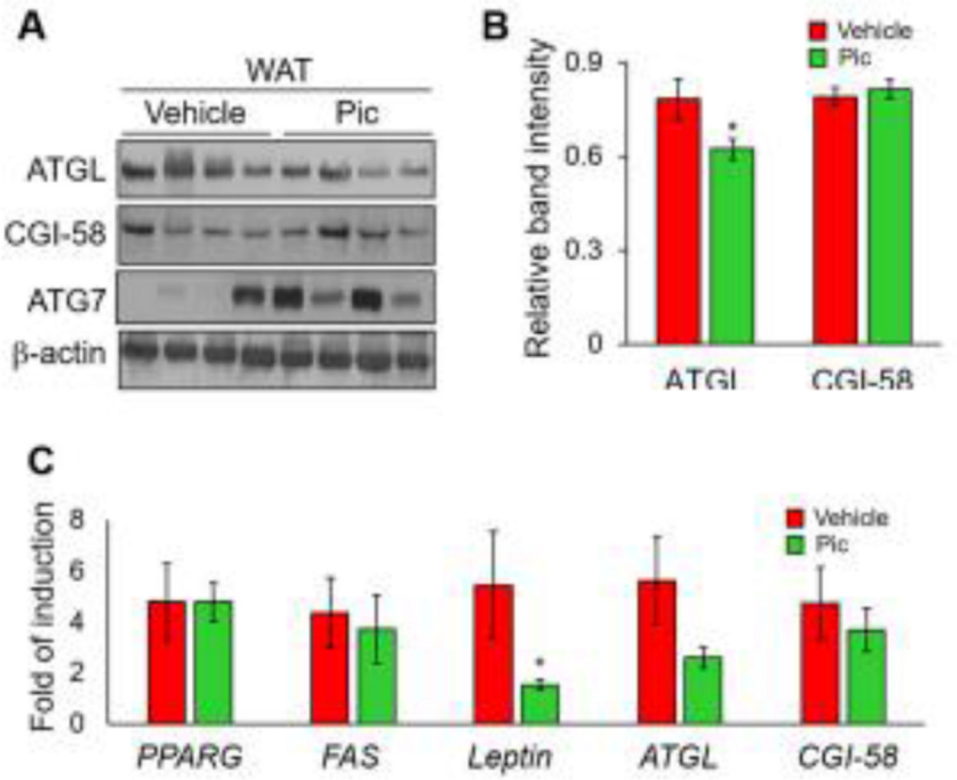

Fig. 6. Piceatannol administration alters high-fat diet-induced expression of ATGL and *leptin* levels in WAT of diet-induced obese mice.

Total proteins and RNA isolated from epididymal WAT of piceatannol-administrated diet-induced obese mice were subjected to Western blot analysis and quantitative RT-PCR for the analysis of ATGL, CGI-58 and ATG7 proteins (**A**, **B**) and mRNA levels of *PPARG*, *FAS*, *leptin*, *ATGL* and *CGI-58* (**C**), respectively. Data in panels **B** and **C** are presented as means ± SEM. (n=3–4, *, $p < 0.05$).